4

Digital Holographic Recording in Amorphous Chalcogenide Films

Andrejs Bulanovs
Innovative Microscopy Center, Daugavpils University
Latvia

1. Introduction

After the invention of holography and development of hologram micro-embossing, mass replication of hologram became possible. Use of a hologram as a security option for valuable documents and products was soon realized and won a large-scale application, which did not hinder development of other security features though. A great variety of other diffractive microstructures commonly known as diffractive optically variable image devices (DOVID) has appeared. Alongside the development of computer technology, digital holographic recording in applied holography has acquired a wide range of application. Nowadays, various types of digital holograms are used for protection and identification of industrial products and documents against counterfeiting, as well as for packing and decorating.

Now two optical technologies for digital recording of protection holograms and DOVID, having similar principle of image formation, are widely used: dot-matrix and image-matrix holographic recordings (Pizzanelly, 2004). A dot-matrix hologram consists of an array of fine diffractive dots holding an image together (**Fig. 1a**). Each dot in such a hologram consists of a uniform diffraction pattern in which the grating pitch and grating orientation

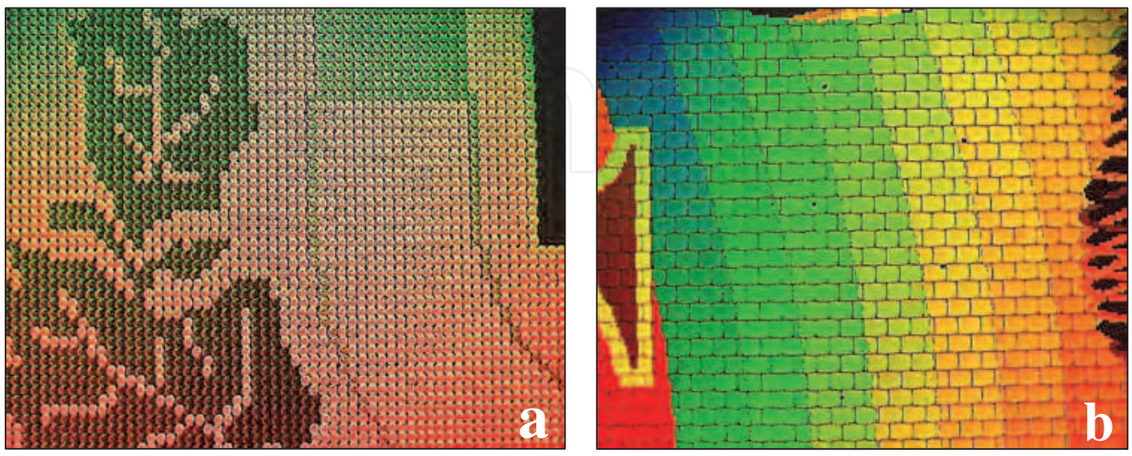

Fig. 1. Photos of microstructure of dot-matrix (**a**) and image-matrix (**b**) holograms recorded on $As_{40}S_{20}Se_{40}$ photoresist.

may vary from dot to dot. In contrast, an image-oriented hologram is composed of an array of microscopic images (**Fig. 1b**). Positive organic photoresists are conventionally used in both technologies for recording relief-phase holograms.

In its turn**,** formation of surface relief in the process of selective dissolution of amorphous chalcodenide films is well known. The phenomenon is based on difference in dissolution rate of the exposed and unexposed areas of chalcogenide film surface in alkali developers (Teteris, 2002). This phenomenon of photo-induced changes in the dissolution rate of a large group of amorphous chalcogenide semiconductor films was the basis for an extensive development of a new class of inorganic resists.

Holographic recording in amorphous chalcogenide films is the subject of investigation for many scientists. In 1970, the first articles about the recording of holographic diffraction grating in the amorphous films As_2S_3 were published. Due to essential photoinduced changes of optical properties, thin films of amorphous chalcogenide semiconductors are very promising media for phase hologram recording. It is worth mentioning that diffraction efficiency of phase hologram in chalcogenide media reached up to 80%, and optical resolution exceeds 5000 mm^{-1}.

Organic photoresists are mainly used for recording relief-phase holograms; they are sensitive enough only in the ultraviolet part of spectra $\lambda < 480$ nm. For lasers with the wavelength λ=400-650 nm, use of photoresists based on chalcogenide films is very promising. Amorphous chalcogenide films have been recently used as a material for holography in visible spectrum ($\lambda \leq 650$ nm) with high resolution (> 5000 lines/mm) and light sensitivity in the range 1-10 J/cm^2.

Successful results of recording holograms on As-S-Se films have long been known. Photoresists based on amorphous chalcogenide films are effectively employed by some holographic companies in the production of rainbow holograms and diffraction gratings. But use of these films for recording dot-matrix and image-matrix holograms has not yet been studied. There seem to be two main reasons for this. First, As-S-Se films have a low sensitivity (~1-20 J/cm^2) in comparison with organic photoresists (~1-100 mJ/cm^2). Second, image-matrix technologies of hologram recording result in great losses of laser radiation energy (up to 99 %) at optical and Fourier filtrations.

To overcome the above-specified problems in recording dot-matrix and image-matrix holograms, a device specially adapted for the use of As-S-Se films has been developed. Optimum modes of optical recording are investigated, and relief-phase holograms with high diffraction efficiency (DE) were recorded by means of the created device. Another positive result was that the time for recording holograms on the As-S-Se based photoresist was comparable to the time for recording them on organic materials.

The present article contains data of an experimental recording of relief-phase digital holograms and DOVID on chalcogenide thin films. The obtained holograms can be duplicated by standard modern technologies.

2. Dot-matrix holographic recording

Intense research into optical characteristics of photoresists based on chalcogenide amorphous glasses has brought about the need for a device that would allow for such materials to be studied and adapted for the use in manufacturing technologies.

An experimental digital dot-matrix (DDM) device for holographic recording was developed and assembled at the laboratory in Daugavpils University. As distinct from the known

DDM devices in which a laser with an intensity modulator and an optical scheme are separate parts, our device has a laser and an optical scheme integrated into one unit. This approach simplifies the overall system construction and adjustment, reduces number of optical components in design and increases reliability. This allows for recording a two-dimensional array of diffracting pixels with preset parameters on the surface of a photosensitive media thus making it possible to produce a holographic image using pixels with parameters that are computer-controlled during the recording.

The fundamental concept of dot-matrix holograms lies in writing the image pixel-by-pixel varying the grating orientation, grating pitch and, if possible, pixel size. Many other approaches to the creation of a similar dot matrix hologram are known. One of them consists in applying laser beam or e-beam lithography to create each grating pixel. Dot-matrix holograms generated by the mentioned type of lithography are commonly referred to as e-beam holograms. They generally achieve an even better resolution and brightness than the mentioned dot-matrix holograms. However, the use of an e-beam machine is extremely expensive. Since the cost of dot matrix holography is much lower than that of e-beam or laser beam holography, it is expected that the former will gain a broad range of application.

A dot matrix hologram comprises a two-dimensional array of micron-sized diffractive elements or pixels. Each element contains a diffraction grating formed by two-plane coherent wave interference. The period of interference fringes is determined by the angle between the interfering laser beams and their wavelength.

The recording is made by converging two focused laser beams to a point of a preset size on the photoresist surface. Thousands of such closely spaced pixels form a dot matrix hologram.

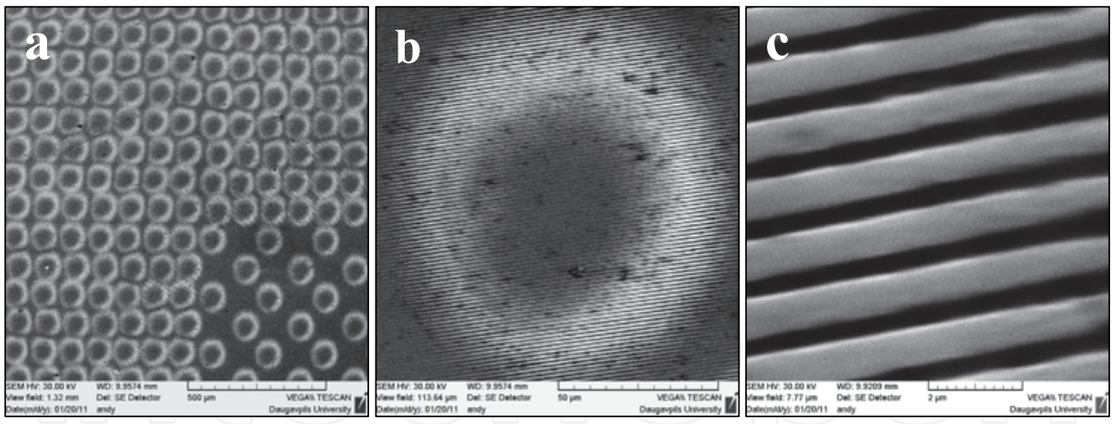

Fig. 2. SEM images of dot-matrix hologram recorded on $As_{40}S_{20}Se_{40}$ photoresist at different magnification. **a**) Structure of a dot-matrix hologram. **b**) Image of one pixel.
c) Diffraction grating in the pixel.

On illumination, each pixel of the hologram diffracts light at a specific angle chosen in the process of making. The angle and the direction in which the diffraction grating of a pixel reflects light are determined by the following two factors:

- Grating orientation in a pixel. This is achieved by rotating the convergence plane of two laser beams before pixel recording.
- The spatial frequency of the grating in pixel. This is achieved by changing the angle between two laser beams.

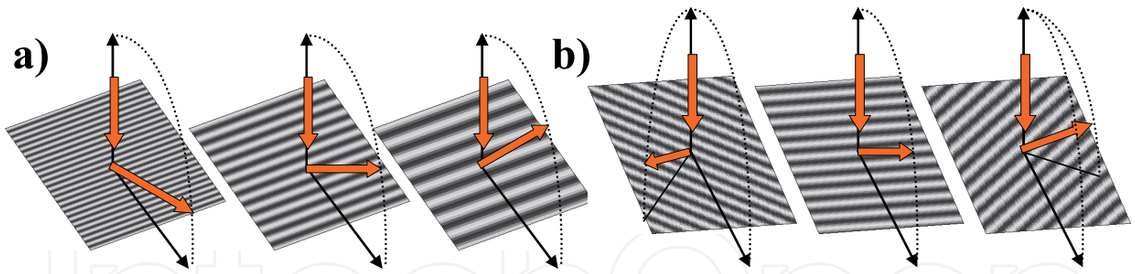

Fig. 3. The changes of the diffraction depend on the period and orientation of the diffraction grating. **a**) Varies the period of the grating. **b**) Varies the orientation of the grating.

By changing the orientation of a grating, the diffracted light can be made skew horizontally left or right with regard to the vertical axis of the initial beam (**Fig.3b**). Only pixels with the same grating orientation are seen in a certain light every time the hologram is rotated. This creates an active 'kinetic' effect, which is difficult to obtain in a conventional holography. The spatial frequency of grating in diffractive pixel determines the vertical diffraction angle (**Fig.3a**). By selecting definite spatial frequencies, each pixel can be assigned a different colour of the visible spectrum. The grating orientation and spatial frequency together determine the wavelength of diffracted light and the direction in which the observer can see the pixel. Each pixel in the computer image usually corresponds to a diffractive pixel in the hologram. The program uses the computer image to calculate the orientation and grating frequency of every element in the hologram according to a developed algorithm. The value of the pixel exposure time is optimized in order to obtain the maximum diffraction efficiency at a given intensity of laser beam. Prior to each exposure, it is possible to set a pause of 10-300 ms.

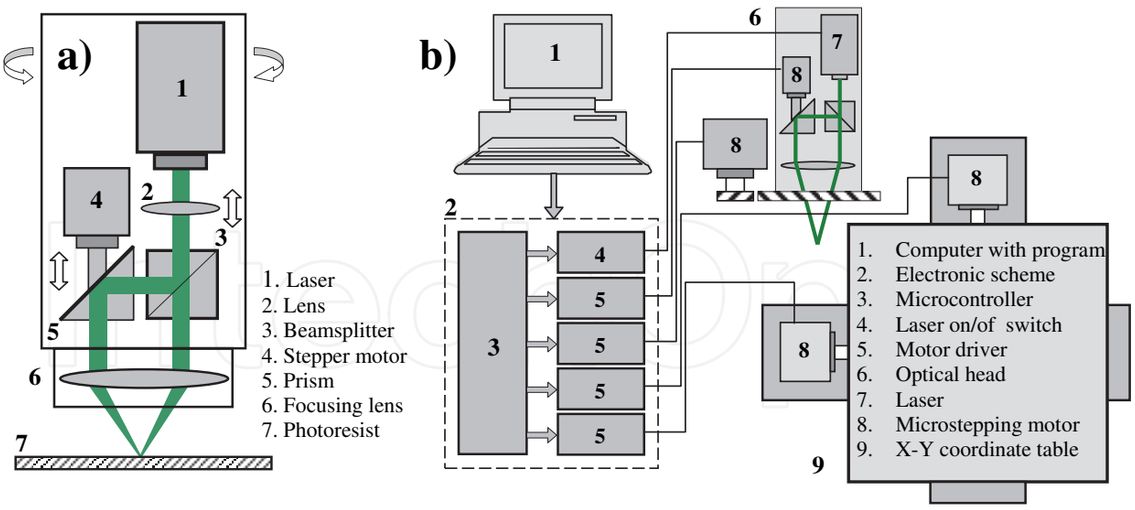

Fig. 4. a) Scheme of the optical head. b) Scheme of the dot-matrix recording device.

This allows for decreasing the vibration that inevitably arises with the use of stepping motors for mechanical moving. The distance between the pixels determines the pixel density and hologram size. The optimal distance is considered equal to the pixel diameter. At smaller distances, pixels overlap, whereas at bigger distances, the pixel density decreases. A significant loss of the diffraction efficiency is observed in both cases.

The overall structure of a dot-matrix holographic recording device and its photo are shown in **Fig. 4b** and in **Fig. 5a**, respectively. A glass plate coated with photoresist is positioned with the help of a accurate coordinate table **9** (see **Fig.4b**).

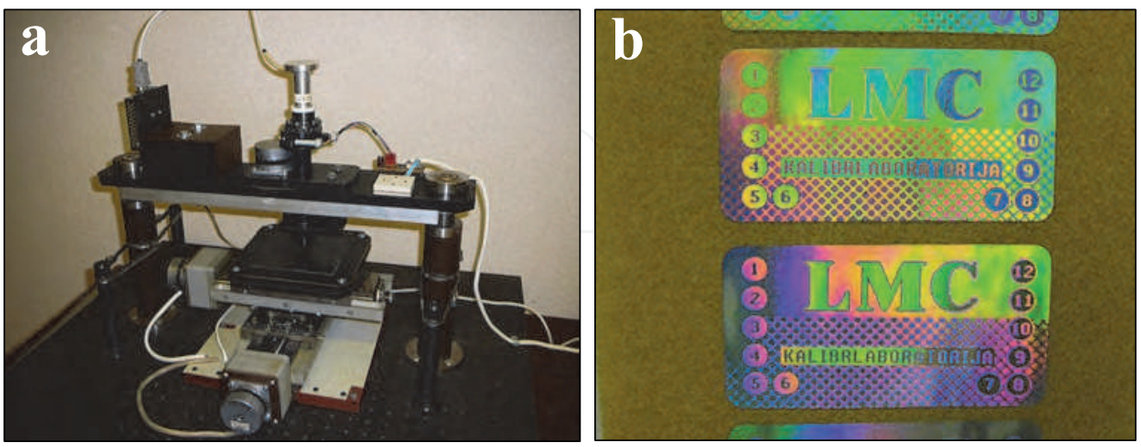

Fig. 5. **a)** Photo of a dot-matrix recording device. **b)** Photo of a protective dot-matrix hologram recorded on $As_{40}S_{20}Se_{40}$ photoresist with the help of the created device.

The size of X-Y movable area was 75/75 mm, and the positional accuracy was about 3 μm. Stepping motors **8** were used for rotating the optical head, moving the reflecting prism in optical scheme for changing grating pitch size. Also stepping motors **8** were used for changing position of the coordinate X-Y table. The permissible minimum level of the motor vibration was achieved by the use of the microstepping motor driver with operation in eighth-step mode (we use A3977 microchip). The electronic module **2** shown in the figure was assembled on the basis of a microcontroller ATMega16, the parts of which were connected with driver microschemes of stepping motors **8** and electronic key of the switching laser **4** (on-off). The electronic module is intended to receive commands and data from the computer **1** via an RS-232 interface and to produce electronic signals on the basis, of the data and commands to control the drivers of subordinate devices. Such coordination of the program with peripherals allows for speeding up and optimizing the calculation of hologram in the main program, whereas the microcontroller program provides the command over all mechanical motion.

An interference pixel with the size of several tens of microns is formed in the rotating optical scheme **Fig.4a.** As a source of coherent radiation, a compact diode pumped Nd: YAG SHG laser (model LSR532-ML50, wave length 532 nm, max. power 50 mW) was used, which can operate in radiation modulation regime by the external TTL signal (frequency of modulation up to 25 kHz). In this case, an exterior electro-optical shutter, which is commonly used with gas lasers, is not needed. For the input of a laser beam in the rotated optical scheme, it is usually necessary to centre the beam along the rotation axis. Also for preservation of constant polarization during the hologram recording it is necessary to use a λ/4 phase plate before and after the input of a laser beam in the optical head **(Fig. 6a)**. The disadvantage of similar designs is complexity of adjustment, a great number of additional optical elements, and necessity of using a symmetric optical scheme. **Fig. 6** shows the fundamental difference between design of created dot-matrix recording device and similar devices

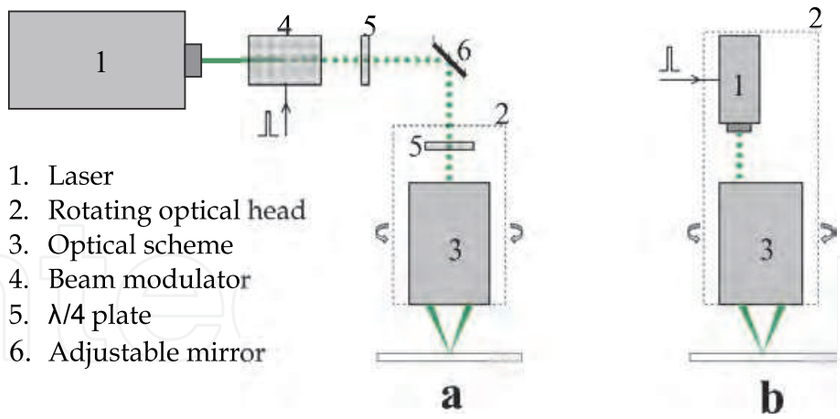

Fig. 6. Entering of the laser beam into a rotating optical part of the dot-matrix recording device. **a)** The laser is located outside of optical scheme. **b)** Laser is integrated into the optical scheme.

Compactness of the laser allowed us to include it in the design of the optical head (**Fig.6b**). Such a design minimised the number of optical elements and enabled utilization of an asymmetric optical scheme, which is very stable and easily adjusted.

Figure **Fig.4a** shows the optical scheme, which was used for the formation of diffraction pixels with preset pitch size and orientation angle. The beam splitter divides the laser beam into two parts, equal in intensity and parallel to the rotation axis, which are reduced with the help of a focusing lens **6** (f=20 mm) and converge in the point of a certain size (30-150 μm). The size of the point is adjusted manually by shifting a far focusing lens **2** (f=300 mm). The stepper motor **4** moves a reflecting prism **5** in the vertical direction and allows for changing distance between the divided beams and, accordingly, frequency of diffraction grating in the pixel within the range of 750-1000 mm^{-1}. The orientation angle of grating in the pixel is changed by turning the optical head.

The disadvantage of this optical design is a considerable path-length difference between the interfering wave fronts (10-15 mm), which imposes stricter requirements on the laser coherence. The coherence length of the used laser radiation was therefore measured with a Michelson interferometer and exceeded 3 cm, which was enough for interference conditions. Rather a large difference of the optical path between beams did not allow us to record pixels less than 30 μm in size because the focusing points of beams are slightly different.

The developed device for dot-matrix holographic recording was successfully used for research purposes and for producing protective holographic labels (**Fig. 5b**).

For recording a dot-matrix hologram, $As_{40}S_{15}Se_{45}$ chalcogenide thin films were used. Films were obtained by thermal evaporation onto glass substrates in the vacuum of ~10^5 Torr. The method of film evaporation in vacuum allows for obtaining homogeneous films on the substrates of different size and form. The effect of light on As-S-Se films gives the possibility to carry out selective etching of differently exposed parts with a great resolution of up to 5000 mm^{-1}; that allows for the use of these films in applied holography. These films possess a differential chemical etch rate between exposed and unexposed areas; the exposed portions have a slower etch rate in non-aqueous amine-base solution due to structural changes. Structural changes arise due to the absorbtion of light with bandgap energy, this results to the creation of the electron-hole pairs, whose subsequent recombinations leads to the processes of atoms bond reforming. The wide spectral sensitivity range of the material (from ultraviolet up to 650 nm) makes the task of choosing a laser easier. Optical recording

on a photoresist and the following chemical etching result in the creation of a relief-phase hologram (**Fig. 7b**).

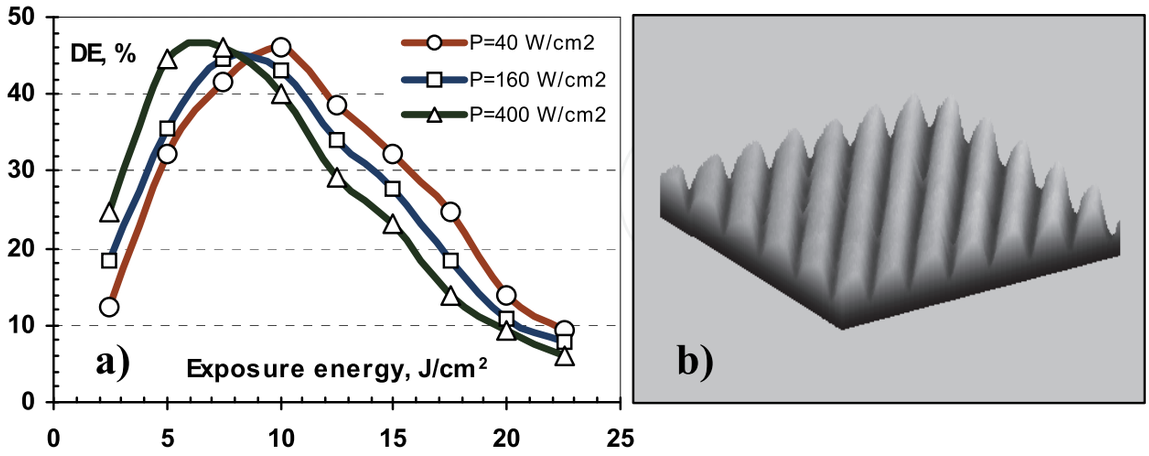

Fig. 7. **a)** Diffraction efficiency of dot-matrix holograms recorded on $As_{40}S_{20}Se_{40}$ photoresist as a function of exposure dose. **b)** 3D model of the gratings profile based on an SEM image.

The relief microstructure of the photoresist surface is copied onto a hard metallic material, usually nickel, by the galvanic method. Once a hologram pattern has been created, the traditional hologram manufacturing process, including electroforming, mechanical recombining, and embossing, can be used in the mass production of holograms.

The diffraction efficiency (DE) of diffraction grating covered by a ~20 nm layer of Al by thermal deposition in vacuum is shown on **Fig. 7a**. Determination of diffraction efficiency was performed at a normal incidence of a laser beam onto the surface of a hologram. The intensites of diffraction light was measured in both first maxima and diffraction efficiency was calculated with the help of the formula $DE=(I_{+1}+I_{-1})/I_0$, where I_0 is an intensity of the incident beam, and I_{+1} and I_{-1} are intensities of the first diffraction maxima.

Relief-phase dot-matrix holographic gratings were obtained in the composition of $As_{40}S_{20}S_{40}$ with the diffraction efficiency about 50%. In course of determining dependence of the DE on exposure, it was observed that sensitivity of the material increased when the exposure power density increases. So at the power density 40 W/cm², the optimum exposure was close to 10 J/cm²; when the power density increases up to 400 W/cm², the optimum exposure decreases approximately twofold, reaching ~ 5 J/cm² (**Fig. 7a**). The Gaussian distribution of intensity in a laser beam gives an uneven distribution of the exposure in a pixel when recording it on a photoresist (**Fig. 2b**). As a result, the effective diameter of pixel changes varying the exposure time. This effect makes it possible to handle the pixel density by a programme when holograms are recorded in spite of certain losses in the diffraction efficiency due to deviation from optimal exposure dose.

3. Image-matrix holographic recording

With the development of spatial light modulators and computer technology, applied digital holographic recording has acquired a wide range of use. After the appearance of translucent

Liquid Crystal (LC) and reflecting Liquid Crystal on Silicon (LCoS) spatial light modulators (SLM) of a new generation, an interest regarding their use in optical schemes for recording computer-generated holograms (CGH) and diffractive optically variable image devices (DOVID) has grown.

An SLM chip has a twisted or parallel-aligned nematic liquid crystal layer to modulate light. It changes the phase and polarization state of the incident light. Parameters of modulation depend on the alignment of the LC and polarization state of the incident light. The LC alignment is controlled, pixel-by-pixel, using DVI (Digital Visual Interface) signals from the computer. Electro-optical effects in liquid crystal displays make them suitable for amplitude and phase modulation of coherent wave fronts so that they can be used as programmable diffractive elements.

After passing through the spatial light modulator, a wave undergoes a local change of the phase and orientation of the polarization plane. The size of the minimum area of the wave front undergoing change is determined by the size of the modulator pixel. The degree to which the wave parameters change depends on the angle between the optical axis of the modulator and polarization direction of a laser beam, as well as on the level of electrical signals on the modulator pixels. Two extreme cases are possible. In the first the modulator changes only the phase of the transmitted wave leaving polarization and amplitude unchanged. This is a phase modulation regime. In the second case, the modulator changes the direction of polarisation plane, with small changes of phase in all sections of the wave front. The wave becomes modulated in amplitude after going through the polarizer.

For recording CGH and DOVID, an image-matrix optical set-up shown in **Fig. 8a** was used.

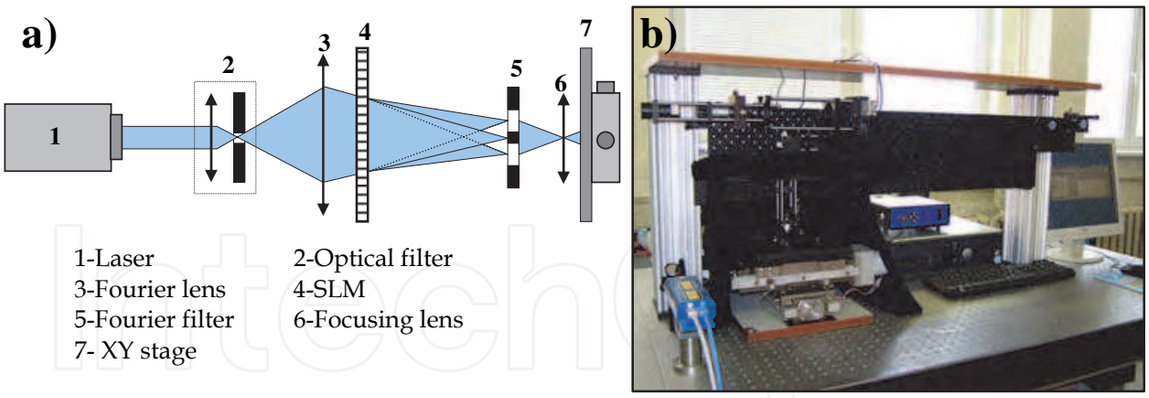

Fig. 8. a) Optical scheme of the image-matrix holographic recording device. b) Photo of the device.

It utilizes a diode laser **1** (100mW, 405nm), whose spatially filtered and expanded beam illuminates a transparent SVGA spatial light modulator **4** located behind the Fourier lens **3**. The lens **3** in the plane conjugated to the pinhole **2** creates the Fourier spatial spectrum of the laser wavefront diffracted on the amplitude-phase image displayed on SLM. Intensity peaks of the spectrum, that are the farthest from the centre, correspond to the higher orders of diffraction. A spatial filter **5** is positioned in the Fourier plane behind the SLM in order to block the zero and higher than first orders. After the inverse Fourier transformation, a

hologram with a doubled frequency of diffraction grate is created with the help of an objective **6** by interference of the I_{+1} and I_{-1} orders of the wave diffracted at the modulator. This means that the image on the photoresist surface for periodic structures is formed only due to the interference of the second harmonics of spatial spectra. For example, if we will send on the modulator the image corresponding to N black-and-white stripes, on the photoresist surface we will get a sinusoidal intensity distribution consisting of 2N peaks. An image is displayed on the SLM then reduced to microscopic size (140x105 μm) by a lens system **6** and recorded on the photoresist plate placed on the XY-stage **7**. An important advantage of such set-ups is that they do not require vibration damping.
A general principle of the formation of a large size hologram is shown in **Fig. 9.** The recording is performed sequentially by rectangular micron-sized areas as shown in **Fig. 9a**. The sections tightly fill the entire area of the hologram, and a human eye does not perceive a discrete structure of the hologram consisting of micron-sized sections. Optical recording of the interference pattern is performed on each individual area of the hologram.

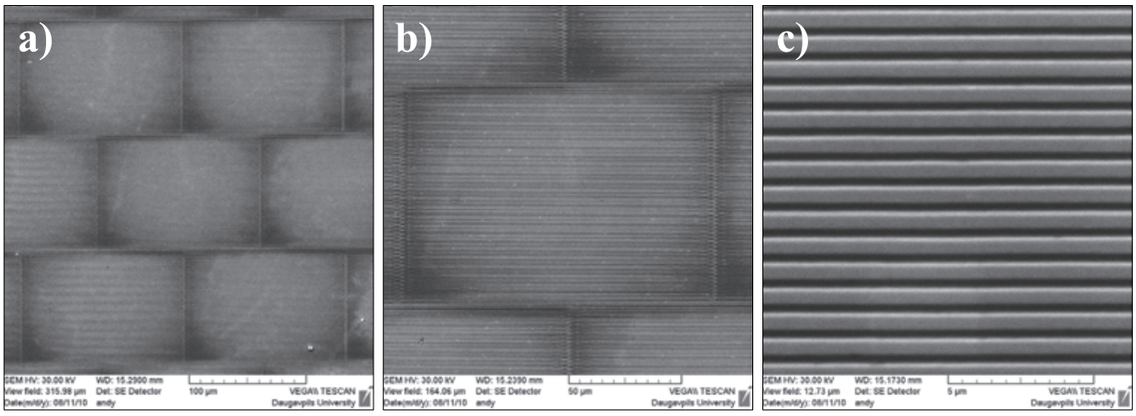

Fig. 9. SEM images of image-matrix hologram at different magnification.
a) Image-matrix structure of hologram. **b**) Image of one frame. **c**) Diffraction grating in the frame.

The pattern is set by the amplitude-phase image on the modulator and corresponds to the graphic figure on the computer monitor. In order to lessen the perceived discreteness of the hologram structure, the neighbouring rows of its micro-images are shifted the length of half-frame relative to each other. Each separate image from the matrix structure contains a computer-generated hologram (CGH); in a simple case, it may be a set of gratings with a grating pitch and orientation adjusted to the requirements (**Fig. 9c**).
The phase modulation regime with Fourier filtration is promising for use in applied holography for it offers a way of obtaining diffraction gratings with the frequency 300-2000 mm^{-1}. The maximal frequency is estimated according to the following formula:
F_{max} =2 n.a./λ , where n.a. is a numerical aperture of objective, and λ is a laser wave length.
The minimum frequency is determined by the size of the central diaphragm (L ~ 1mm) in the mask **5**, which blocks the zero order of diffraction and is calculated by the formula $F_{min}=L/(\lambda f)$, where λ is a laser wave length, f focal length of the objective **6**, and L size of the central diaphragm.

Lessening the laser energy losses in case of an optimal optical scheme and reducing the frame area two times in comparison with the conventional (200x150 μm) one allowed for a considerable increase of illumination intensity comparing to analogous devices employing organic photoresists. This, in its turn, made it possible to record holograms on chalcogenide films of low sensitivity without any considerable loss of rate.

In many practical cases the principle of formation of the holographic image with the help of image-matrix technology is close to the dot-matrix technology considered above. The recording of the image-matrix hologram is made by frames of a certain size which depends on the adjustment of optical system. Every frame contains an array of diffraction pixels, which fill all of the frame area and usually have a square form. A diffraction grating with the given period and orientation or functional microstructure (for example, shown in Fig. 15) is recorded in every such pixel.

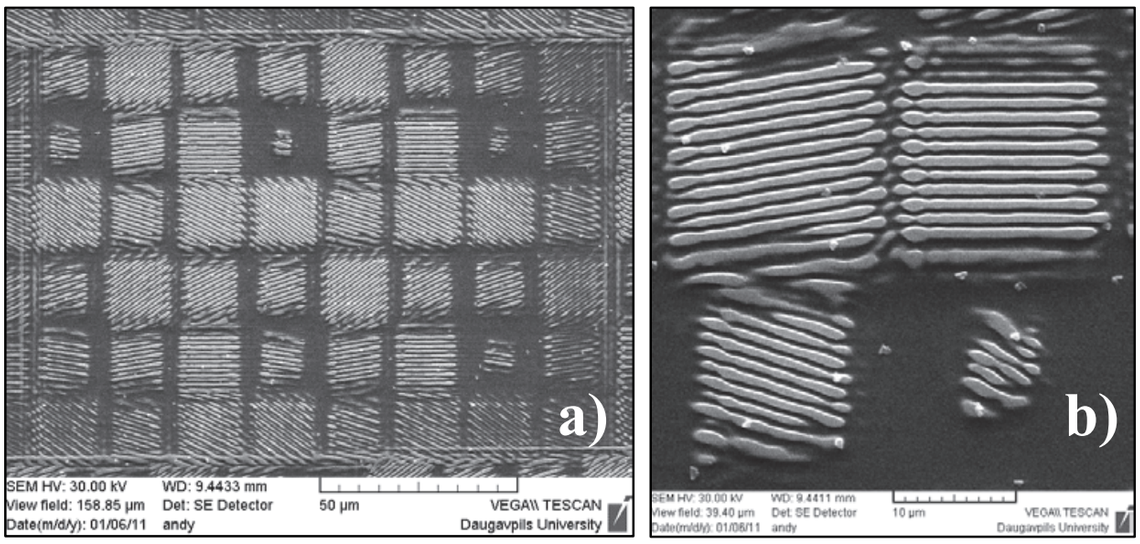

Fig. 10. **a)** SEM image of one frame with the matrix of 8x6 different pixels. **b)** SEM image of pixels with different grating orientation and modulated by size.

When the pixel size changes, its relative visual brightness varies. This perception is useful for recording of grey-scale images or photos. The programmed realization of kinetic visual effects is possible when the turn of the hologram results in the change of visible images. Another example is the possibility of imitating three-dimensional images when an individual image is formed for each eye according to the changed viewing angle of an object (perspective).

Fig. 10a shows a SEM image of one frame of the stereogram containing 9 combined images for creating an illusion of a 3D object. In this case, each frame consists of an array of 8x6 pixels of size 15 μm. Every pixel in the array corresponds to a graphic point in one of the combined images. Each of the combined images is visible from a certain angle which is determined by the orientation of diffraction grating of pixels, appropriate to this image. The size of a pixel is proportional to a level of grey color of the appropriate graphic point (**Fig. 10b**). Realization of a holographic image in real colors is also possible. In this case, each dot of the graphic image corresponds to three diffraction elements and an R-G-B model of the basic color mix is realized in the direction of the observer.

The designed and assembled device for image-matrix holographic recording was successfully used for research purposes as well as for producing holograms for the

protection and identification of industrial products and documents. A sample of image-matrix hologram recorded on inorganic As-S-Se photoresist is shown in **Fig.11b**. Optimization of the relief formation processes makes it possible to produce gratings with high values of diffraction efficiency. A 3D model of grating profile corresponding to the DE~50% is shown in **Fig.11a.**

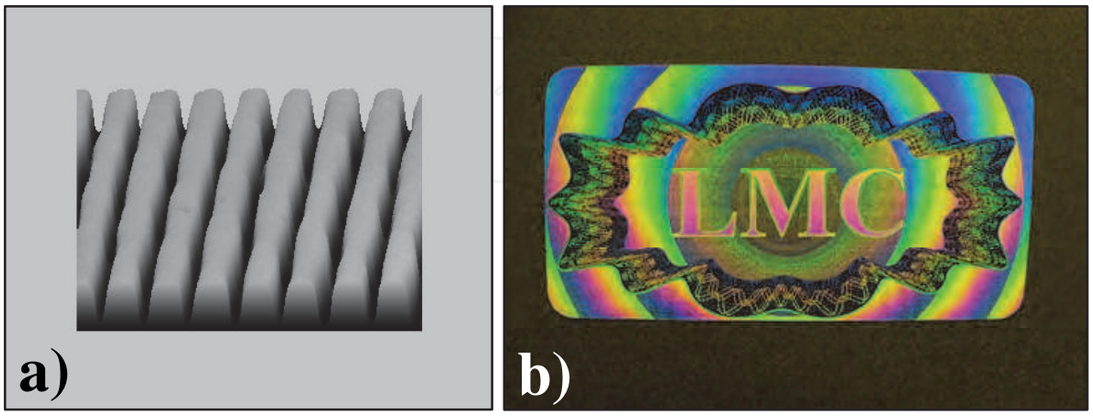

Fig. 11. **a)** 3D model of the gratings profile based on a SEM image. **b)** Photo of a protective image-matrix hologram recorded on $As_{40}S_{20}Se_{40}$ photoresist with the help of the created device.

For recording an image-matrix hologram, we used a $As_{40}S_{15}Se_{45}$ chalcogenide thin film and organic photoresist of the AZ1800 series. Micro relief of the hologram surface in these cases is shown in **Fig. 12**.

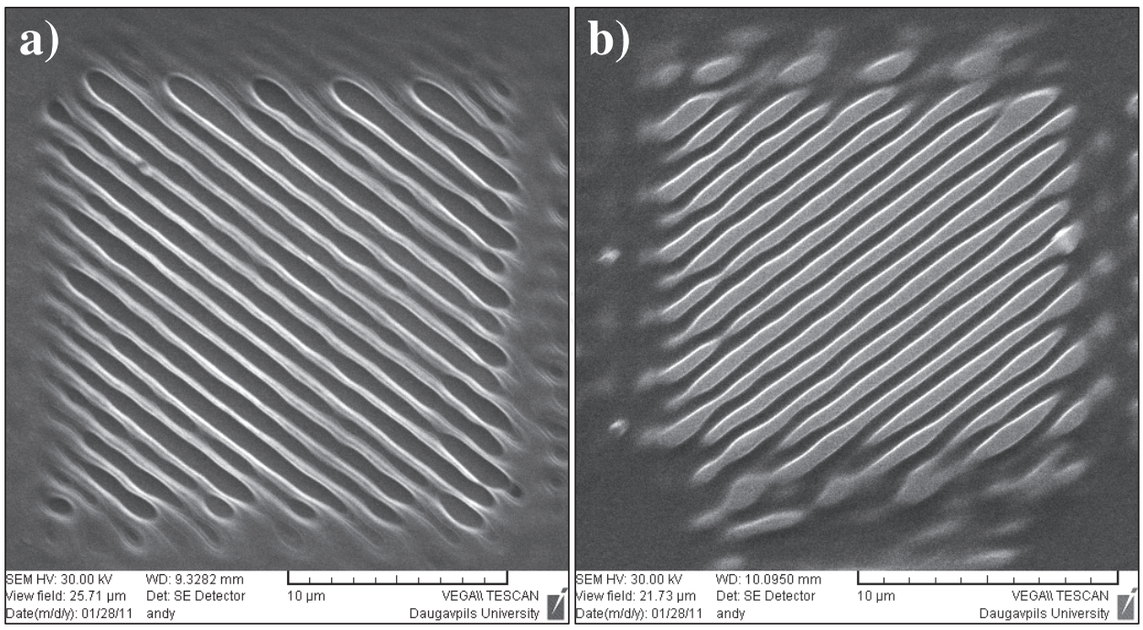

Fig. 12. SEM image of pixel with diffraction grating recorded by image-matrix technology **a)** positive organic photoresist of the AZ1800 series **b)** inorganic negative $As_{40}S_{20}Se_{40}$ photoresist.

Evaporated As–S-Se films undergo photostructural changes in the regions exposed to the light of the energy higher than the bandgap energy. When the thermal deposition method is used, the vapours are condensed on a room-temperature substrate, the chemical reactions among the fragments of the original compounds are not quick enough, and the high-temperature state is then partly or fully fixed and preserved. A micro-heterogeneous film, which is far from thermodynamic equilibrium, is then obtained. Exposure of such films can induce photochemical reactions, e.g. polymerization or depolymerization among individual fragments of the film, changes of local structure, and, as a result, change the chemical reactivity, i.e. dissolution rate in various alkaline and base organic solvents. After exposure, the samples were chemically treated in non-water amine-based organic solutions (negative etching) to form a relief pattern.

When placed in an appropriate solvent, the exposed areas of the film are protected from the etchant in proportion to the irradiation dose. The dependence of etching speed on the exposure dose of such negative wet etching is shown in **Fig. 13**, where the exposed parts of the samples are more resistant to the amine-based solvents than the unexposed regions. The highest selectivity of etching can be achieved after 2 J/cm² of exposure. A longer exposure slightly increases the etching ratio.

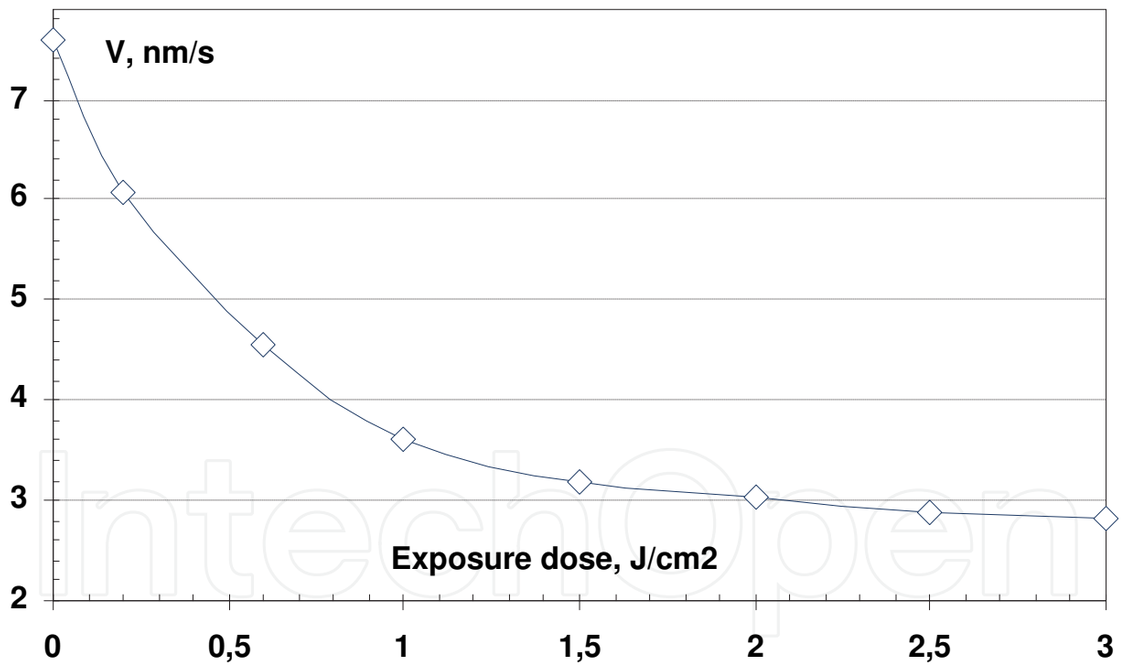

Fig. 13. Dependence of etch rate of $As_{38}S_{20}Se_{42}$ films in non-aqueous amine-base solution on exposure (λ=405 nm).

The effect, whereby the speed with which amorphous As-S-Se films undergo chemical etching, directly depends on the exposure dose, allows for obtaining relief-phase holograms suitable for mass production by conventional technologies and widely used in applied holography.

For relief depth of ~ 150 nm (λ/4 for wavelength 550nm) photo induced structural changes in the film surface layer i.e. the layer that actually undergoes chemical etching, which is ~

250 nm thick, are necessary. In such a case, it appears optimal to use a laser with the wavelength corresponding to the section of the As-S-Se film spectrum with a low optic penetration (λ= 400-550 nm for $As_{38}S_{20}Se_{42}$ films) in order to minimize the exposure time; a higher penetration results in a lower photo induced changes at the film surface.
For obtaining reflective relief-phase holograms on As-S-Se films, lasers with wavelengths 400-650 nm can be used. But for a higher speed of recording image-matrix holograms, it is preferable to employ short wavelength lasers. The smallest depth of structural changes corresponding to λ=405nm is sufficient for obtaining relief-phase holograms with the required depth of micro-relief by means of selective etching.
The experimental curves showing dependence of diffraction efficiency on exposure dose for different grating frequences can be seen in **Fig. 14**. The maximum values of diffraction efficiency are approximately equal for all grating frequences and reach 55-65% in exposures in the range 0.8-1.1 J/cm².

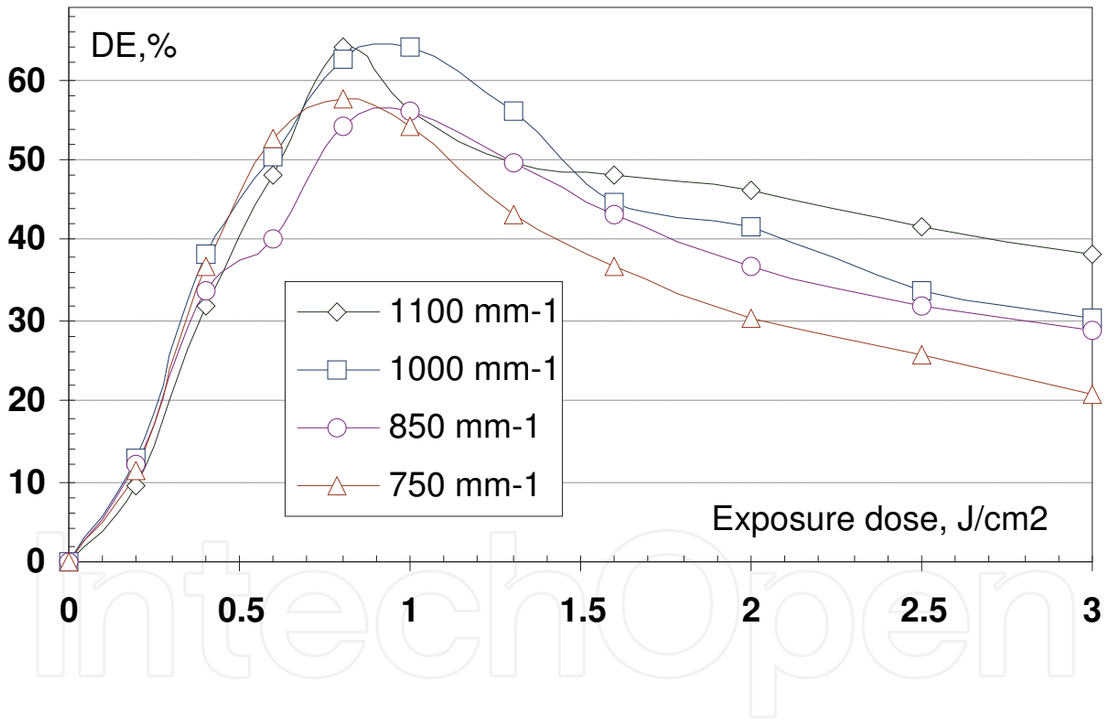

Fig. 14. Dependence of diffraction efficiency of image-matrix hologram on exposure dose at different grating frequencies.

One of the major advantages of image-matrix technology over other ones is that it allows for recording a huge amount of microstructures that differ from simple diffraction gratings. They can be used as additional security elements embedded in holograms. **Fig. 15** shows some relief microstructures that were recorded on As-S-Se photoresist with the help of image-matrix technology. The structure of resist relief was investigated by using a scanning electron microscope.

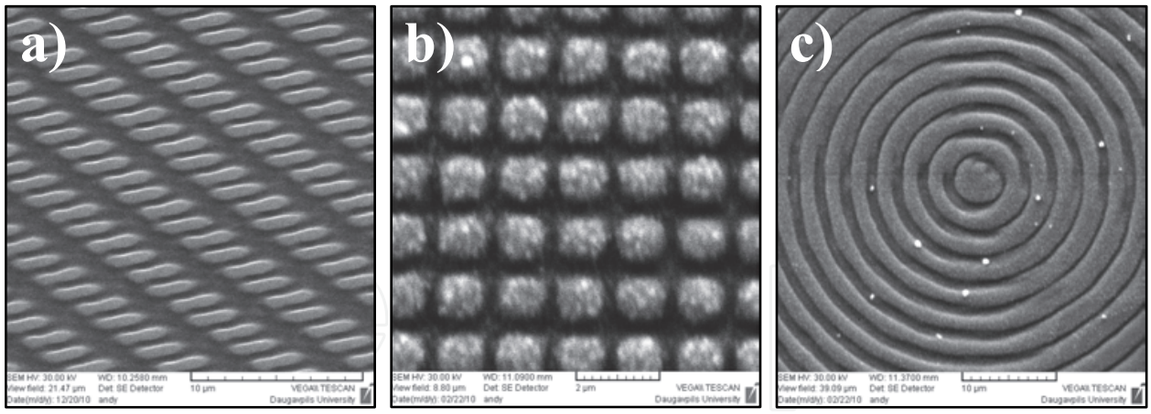

Fig. 15. Samples of microstructure that were recorded on As-S-Se photoresist with the help of image-matrix technology: **a**) complex grating, **b)** 2D diffraction grating, **c)** axicon.

4. Image-matrix recording device based on LCoS spatial light modulator

At the current state of technological development, LCoS (Liquid Crystal on Silicon) optical modulators have characteristics excelling those of the modulators created by the LCD (Liquid Crystal Display) and DLP (Digital Light Processing) technologies. From the point of view of their practical application, LCoS devices have the best of such important parameters as small pixels (down to 8 μm), a great number of pixels (HDMI resolution), high fill factor (till 95%), high frame rate (up to 180Hz), high reflectivity (better than 70%), weakly coupled amplitude or phase modulation, high contrast, and depth of phase modulation above 2π in the visible range. These improved parameters of recent LCoS displays make them appropriate for high quality digital holography and many other related optical applications.

Fig.16 shows a picture and a overall scheme of the experimental setup for holographic recording using the LC-R 2500 LCoS modulator. The basic principle of the operation is the same as described in third part of the chapter. With the help of the aligned mirror **2**, radiation of the laser **1** is delivered onto the optical filter **4**. The λ/2 plate **3**, placed in front of the optical filter, makes it possible to vary the angle of the laser beam polarization relative to the modulator **6** optical axis.

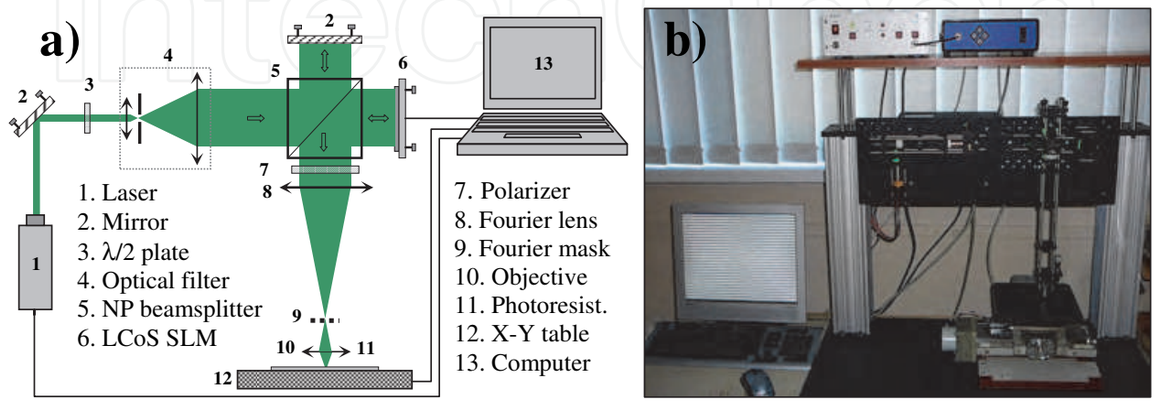

Fig. 16. The scheme (a) and photo (b) of the experimental setup.

The widened and spatially filtered laser beam with a flat wave front falls on the non-polarizing beam splitter **5** (with the coefficient of amplitude division 50/50). The first part of the split beam is incident on the optical modulator LC-R 2500, and after reflecting from its surface, undergoes a local change of phase and polarization plane in accordance with the image on the computer monitor. After reflecting from the mirror **2**, the second part of the beam is used as a reference beam in the interference mode for transition from phase to amplitude modulation of the wave front in optical recording.

The modulation regime (amplitude and phase) is determined by the configuration of the optical scheme (**Fig. 17a, b**), as well as by the position of the polarizer **7** and by the angle between laser radiation polarization plane and modulator optical axis. The long focal length lens **8** (f = 450 mm) forms in its focal plane the Fourier spatial spectrum of the laser radiation diffraction on the SLM image. The mask **9** is situated in the focal plane of the lens **8** and is meant for modifying the Fourier spectra. The inverse Fourier transformation is performed by a micro objective lens (50x, n.a. = 0.5, f = 3.6mm) **10** onto the surface of a plate with photoresist **11**. A compact diode pumped SHG ns laser (model STA-01SH, λ=532 nm, P=50 mW) modulated electronically through TTL signals was used in the optical scheme. In order to form sequential light impulses with a given energy, a regime of the laser **1** operation with generation of optical radiation by external synchronizing pulses is used. Laser pulse with duration ~1 ns and energy ~1.5 μJ corresponds to one external TTL synchronizing pulse. Optical exposure is obtained by a series of electric synchronizing pulses with repetition rate 30 kHz. In the amplitude modulation regime (**Fig. 17a**), polarization of the incident laser radiation coincides with the optical axis of modulator, and the orientation angle of the polarizer relative to SLM optical axis is $\beta=90^0$. After reflection from the SLM surface, at the local area of the wave front the polarization plane is rotated proportional to the signal on the of the modulator pixel. While going through the polarizer **7**, the wave front undergoes amplitude modulation.

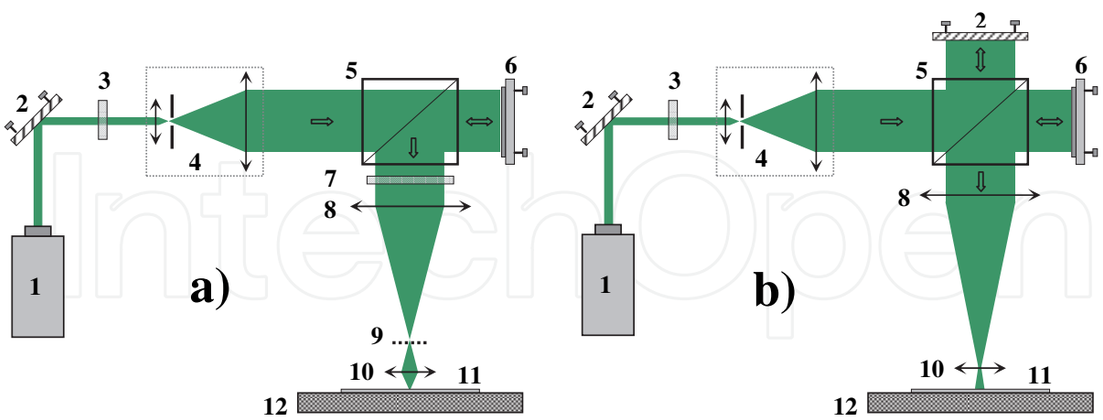

Fig. 17. Optical schemes corresponding to different modes of operation.a) Regime of wave front amplitude and phase modulation. **b)** Amplitude modulation by the phase contrast method.

After the direct and inverse Fourier transformation, which is performed by the lens **8** and objective **10**, the wave front is projected on the photoresist surface with the about 120 times minimization for forming a frame. To form an image in the frame, the full Fourier spectrum

is used and in this case the mask is absent. The amplitude modulation regime allows for recording holograms with a given profile of diffraction grating (rectangular, triangular, sinusoidal, etc.) and frequency ~ 0-800 mm^{-1}.

In the phase modulation regime (also **Fig. 17a**), the polarization plane of the incident wave is at angle $\alpha=25^0$ with the optical axis of modulator and the polarizer is orientated at the angle $\beta=145^0$. In this regime, the polarization of wave front reflected from the modulator undergoes slight changes of direction. After the polarizer, the intensity changes by not more than by 20% of the maximum. The changes of phase in the range from 0 to 2π are proportional to the level of the incoming signal. The mask **9** blocks the zero diffraction order and the orders higher than the first one.

After the inverse Fourier transformation, as it was described in section **3**, a hologram with a doubled frequency of diffraction grating is created with the help of the objective **10** by interference of I_{+1} and I_{-1} orders of the wave diffracted on the modulator. A polarizer **7** is not needed in this case. The phase modulation regime with Fourier filtration is promising for use in applied holography for it gives an opportunity to obtain diffraction gratings with frequency 300-2000 mm^{-1}.

Interference techniques for phase visualisation are shown in **Fig. 17b**, where the signal and reference beams travel along the same optical axis and interfere in the output of the optical system. In this case, the LCoS modulator works in the phase modulation regime. A reference wave front allows for the visualization of phase information in the original wave front.

The common path interference method is also known as the phase contrast method. From the point of view of Fourier optics, a reference beam in the focal plane of the lens **8** changes amplitude and phase of the zero order component in the Fourier spectra of the diffracted object wave, and the SLM image after the reverse Fourier transformation on the photoresist surface by the objective **10** has an amplitude component changing in proportion to the initial phase. Another way of realizing the phase contrast technique allows for visualization of phase perturbations by the use of the Fourier plane phase shifting filter **9** as shown in **Fig. 17a**. In this case, an efficient filter might have near to 100% transmission and a $\pi/2$ phase shift in the central region. But making such a filter in laboratory conditions is a technologically difficult task.

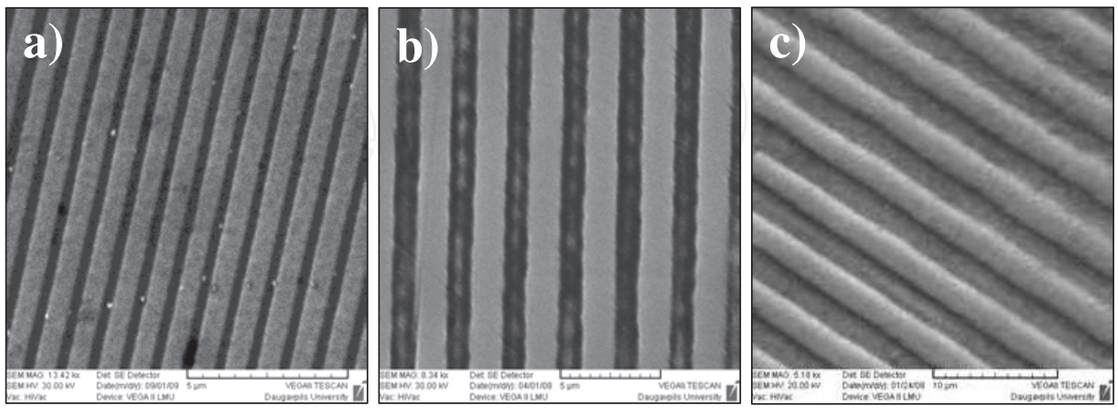

Fig. 18. SEM images of diffraction gratings recorded in different modes of operation on $A_{40}S_{20}Se_{40}$ thin films: **a)** phase modulation regime with Fourier filtration (period 1 μm), **b)** amplitude modulation regime (period 2.5 μm), and c**)** phase contrast method (period 5 μm).

5. Dot-matrix holographic recording on As_2S_3-Al films

For the recording of relief-phase holograms, organic photoresists are mainly used; they are sensitive enough only in the ultraviolet part of spectra $\lambda < 480$ nm. For lasers with the wavelength λ=480-630 nm, it is possible to use chalcogenide film photoresists. Due to the high values of the photo-induced changes of optical properties, the thin films of amorphous chalcogenide semiconductors make a very promising medium for holographic recording. But the use of such films for recording dot-matrix holograms is complicated because of the low sensitivity E=5-30 J/cm². For example, the time for producing dot-matrix holograms consisting of 10^6 pixels is measured by tens of hours. That is why a possibility of increasing sensitivity of films As_2S_3 in the system As_2S_3-Al was studied. Usually, in order to get a relief hologram, a film of photoresist is put onto the substrate with an absorbing layer. In this case the interference pattern in the photoresist layer is made only by incident waves. The interference pattern in the As_2S_3-Al system during the holographic recording can be considered as a sum of incident waves and those reflected by the aluminum sub layer. In case of their overlap, the maximum diffraction efficiency (DE) and sensitivity of the medium are obtained. One of the main conditions for coincidence of interference patterns of incident and reflected waves is equality of incidence angles upon the film surface. If this condition is met, any one of the incident beams after reflecting by the aluminum layer goes in the direction of the incidence of another one (**Fig. 19**). Optical schemes having equal incidence angles of beams are mainly used for the dot-matrix and image-matrix holographic recordings. Taking into consideration the possibility of selective etching of As_2S_3 films, the As_2S_3-Al system is promising from the point of view of obtaining relief-phase holograms.

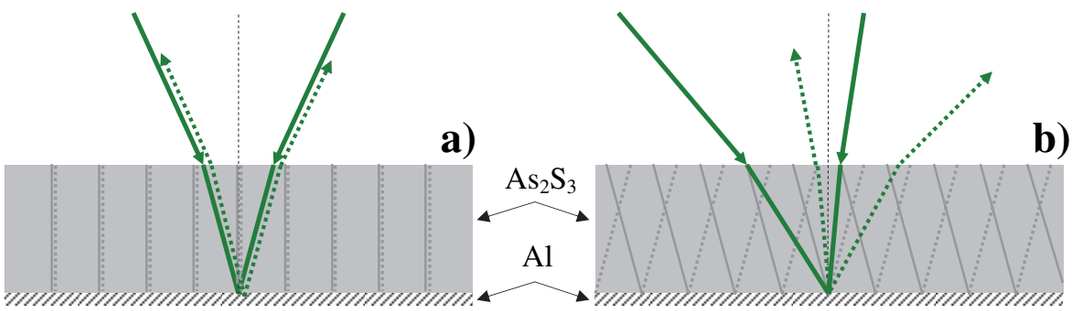

Fig. 19. Scheme of interference field in As_2S_3-Al films.
a) The incidence angles are equal. **b)** The incidence angles are diffrent.

Interference pattern of reflected waves is less stable in time, since before the interference the waves pass the As_2S_3 layer, which has some changes of optical properties during exposure. The aim of the experiments was to determine the conditions ensuring the maximum overlap of interference patterns of incident and reflected waves. A relatively easy way of obtaining the minimum reflection coefficient in a definite part of spectra is viewed as an important feature of the system As_2S_3-Al. Monitoring interference minimum of reflection during the evaporation of film makes it possible to get the system As_2S_3-Al with a minimum value of initial reflection, i.e. 10-15%. Thus, maximum energy absorption of incident waves is obtained and, as a result, the sensitivity of composition during the recording of dot-matrix holograms increases up to 40%.
As_2S_3 films were obtained by thermal evaporation in vacuum onto aluminum (~100 nm) coated glass substrates. The thickness of the As_2S_3 film was closely controlled during the

process of evaporation. Monitoring reflectivity with the interference technique at the wavelength of 532 nm during evaporation of the As_2S_3 layer allowed for obtaining a As_2S_3-Al pattern with the initial reflection of 10-15%. The process of evaporation was stopped immediately as soon as the interference minimum of reflection was reached.
Laser irradiation of As_2S_3 films causes modulation of optical refractive index, which brings about modification of interference conditions, that is modification of the reflectivity coefficient of the As_2S_3-Al system. It was experimentally established that the minimum value of reflection coefficient in the As_2S_3-Al system depends on the thickness of As_2S_3 film and reaches R_{min}=10% at d=2.4 μm (**Fig. 20a**). Dependence of the pixel hologram DE on film thickness is presented in **Fig. 20b**. The maximum diffraction efficiency DE ~40 % was obtained when the film thickness was d=2.4 μm (**Fig. 21**). With an increase of the film thickness, absorption in the As_2S_3 layer at the wavelength λ=532 nm becomes high and lessens the influence of Al-reflected waves on the formation of the interference pattern. In the case of thick films (d > 5 μm), holographic recording takes place only due to interference of incident waves.

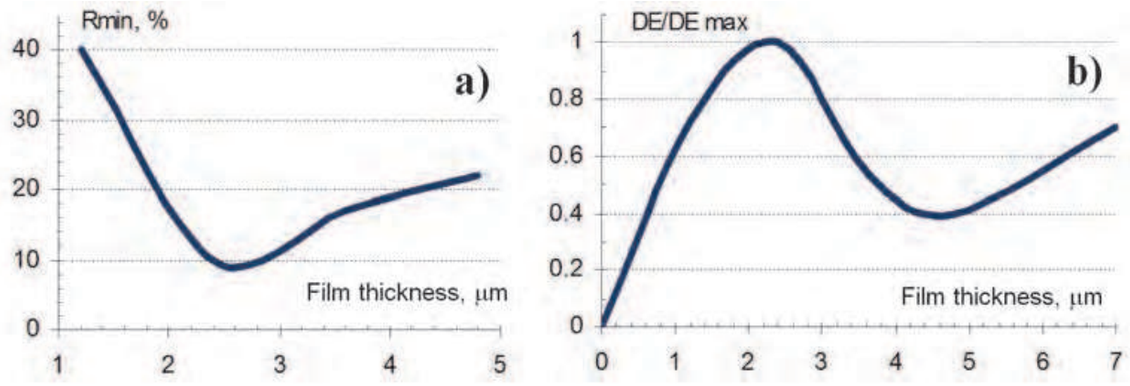

Fig. 20. **a)** Dependence of minimum reflection R_{min} of the system As_2S_3-Al on the film thickness (λ=532 nm). **b)** Dependence of the maximum diffraction efficiency of dot-matrix holograms on the thickness of films As_2S_3-Al

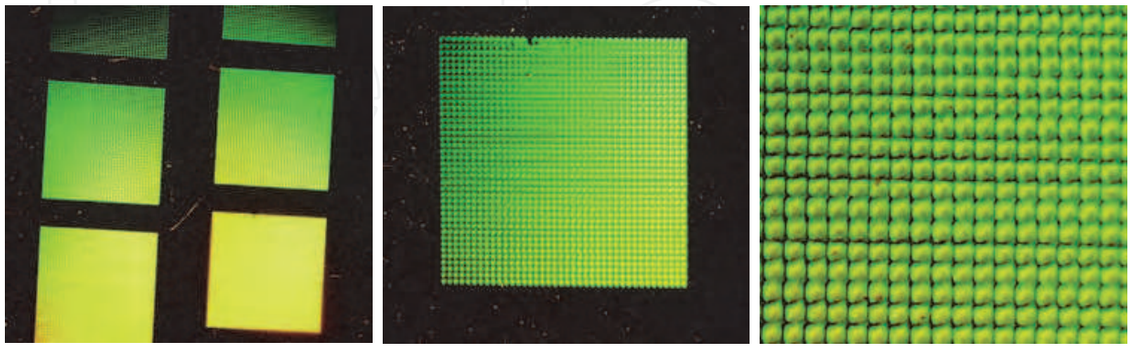

Fig. 21. Photos of the test dot-matrix holograms recorded on As_2S_3-Al films at different magnifications.

During holographic recording, local changes of optical properties of the recording medium, corresponding to the distribution of interference maxima, take place. Changes in local

absorption make it possible to observe the result of holographic recording in thin films. The interference pictures in As_2S_3-Al films of different thickness after the recording of dot-matrix holograms are shown in **Fig. 22a-e**. As seen in **Fig. 22c,d,** two systems of interference bands have equal periods and are mutually shifted. One system of bands corresponds to the interference of incident waves; the other one corresponds to the waves which are reflected from the aluminum surface. Interference maxima of the incident and reflected waves in the films of thickness 2.4 μm are situated very near to each other (see **Fig. 22c**). This case corresponds to the maximum diffraction efficiency of a holographic pixel recording. The optimal exposure for the recording of holograms in the As_2S_3-Al system is E=12-15 J/cm^2. This half that needed for the As_2S_3 films of the same thickness on substrates with absorbing layer of iron oxide. There are two factors significantly influencing the sensitivity of the As_2S_3-Al system during the recording of dot-matrix holograms.

The first is reduction of exposure dose due to superposition with matching of interference patterns for the incident and Al layer reflected waves. This happens when the film thickness is ~2.4 μm (λ=532 nm). The second factor is the possibility of production of As_2S_3-Al films with the minimum reflection coefficient in the part of spectra where the optical recording is made. The main problem in practical implementation of the As_2S_3-Al system in dot-matrix holography is that of depositing an As_2S_3 layer of high uniformity on large substrates.

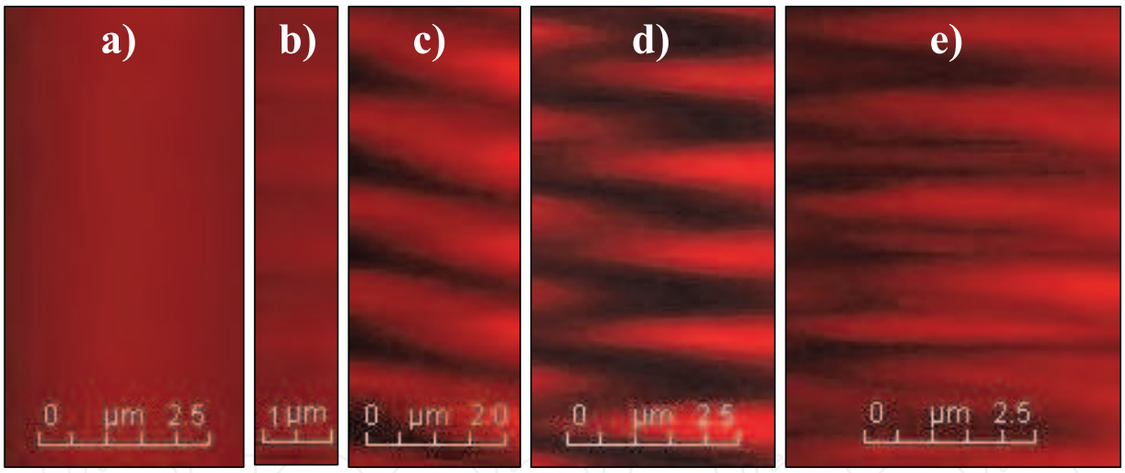

Fig. 22. Image of optical absorption in volume of As_2S_3-Al films after dot-matrix hologram recording (λ=532 nm, N=800 mm^{-1}, E=10 J/cm^2). The pictures were obtained while performing Z-scanning (λ=632 nm) by the confocal microscope LEICA TCS SP5. The left part of each picture corresponds to the layer Al, the right one to the film-air surface; **a)** without recording, **b)** film 1.2 μm, **c)** film 2.4 μm, **d)** film 3.6 μm, **e)** film 4.8 μm.

6. Calculation principles for dot-matrix holograms

The principle of dot-matrix holography is based on decomposition of a hologram image into a two-dimensional array of elementary pixels containing diffraction gratings with parameters that need mathematical calculation. Their size usually lies in the range of 10-100 μm and depends on the technology of optical recording that is used. In each elementary pixel of the hologram there is a diffraction grating with certain period *d*and orientation

angle φ relative to horizontal axis in the plane of hologram (**Fig 23a.b**). Size and shape of pixels may also change. The shape influences the fill factor of the whole hologram. For example, the fill factor of rectangular pixels can reach 100% and for round ones it is only 80%. In the former case, consequently, the diffraction efficiency of the hologram will be about 20% higher than in the latter. It is possible to modulate diffracted light intensity by changing the size of pixels or exposure time during optical recording.

The calculation task is to define the condition that a particular pixel of a hologram would direct a given spectral part of diffracted light towards the observer. The observer can see diffracted light from each element of a hologram only at a certain angle; and the total perception of diffraction of all elements makes a visual effect that corresponds to the initial graphic design. It is obvious that the main factors for reconstruction of the whole hologram are orientation and period of diffraction grating in each pixel, as well as position of an observer and the light source during the reconstruction. In these conditions, the holographic image will correspond to the initial graphic design. If the positions of an observer and the light source are defined, period d and orientation angle φ (Fig. 23a) of the grating completely determine the conditions when an incident white light can be diffracted with the given spectral region towards the observer. In this case, the color of the hologram element corresponds to the color of a dot in the initial graphic image.

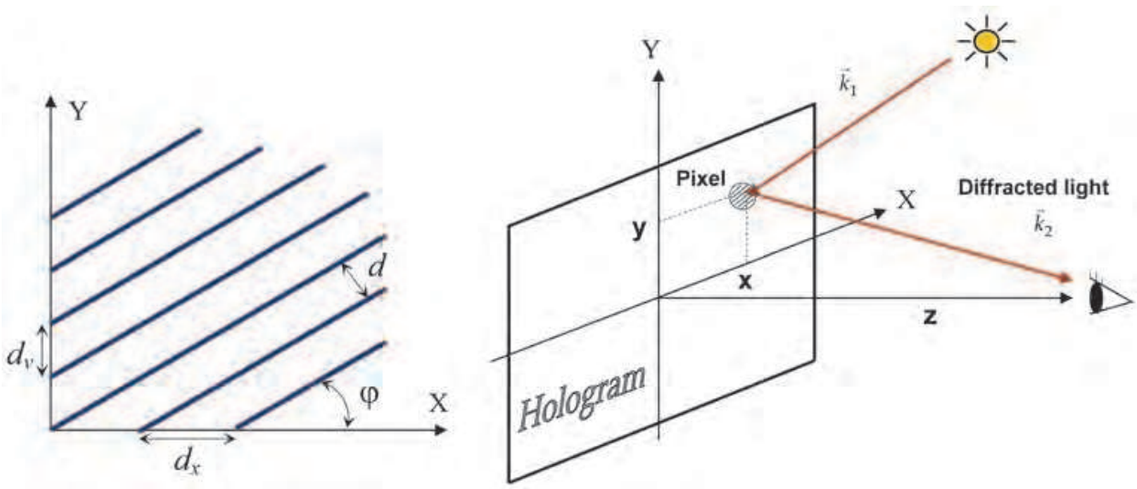

Fig. 23. **a)** Parameters of diffraction grating. **b)** An image element formation by diffraction pixel.

The coordinate system XYZ is chosen in such a way that the hologram is lying in the plane XY, and the Z axis directed to the observer from the center of the hologram (Fig. 23b). Assume that the observer's eye is on the Z axis at the distance of about 30 cm. The light source illuminating the hologram has a continuous spectrum in the visible region, and the direction of the incident radiation is given by the unit vector $\vec{k}_1$. We must define the parameters (d,φ) of the diffractive pixel with the coordinates (x, y), which the observer can see in the color with the wavelength λ_0. If the light with the wavelength λ falls on a flat diffraction grating along the unit vector $\vec{k}_1 = (\cos\alpha_1, \cos\beta_1, \cos\gamma_1)$ the direction of diffraction, which is defined by the unit vector $\vec{k}_2 = (\cos\alpha_2, \cos\beta_2, \cos\gamma_2)$, can be determined by the formulae (Yaotang et al., 1998):

$$\cos\alpha_2 = \cos\alpha_1 \pm \frac{\lambda}{d_x};\ \cos\beta_2 = \cos\beta_1 \pm \frac{\lambda}{d_y};\ \cos\gamma_2 = \sqrt{1 - \cos^2\alpha_2 - \cos^2\beta_2} \quad (1)$$

We will make calculations in order to form image in the +1 order of diffraction. We take the position of a point source with continuous spectrum of light in the plane YZ. If the angle between the Z axis and direction from the light source to the hologram center is θ, then $\vec{k}_1 = (0, -\sin\theta, \cos\theta)$, where the change of the Z-component of incedent light after reflection from the hologram surface is taken into account. The direction of the +1 diffraction order from the pixel with the coordinates (x, y) to the eye of the observer is defined by the unit vector $\vec{k}_2 = (-\frac{x}{L}, -\frac{y}{L}, \frac{z}{L})$, where $L = \sqrt{x^2 + y^2 + z^2}$ is the distance between the pixel and the eye of the observer. Taking into account the above mentioned conditions, the formulas in (1) will look like the following:

$$\cos\alpha_2 = -\frac{\lambda \sin\varphi}{d};\ \cos\beta_2 = -\sin\theta + \frac{\lambda\cos\varphi}{d};\ \cos\gamma_2 = \sqrt{1 - \cos^2\alpha_2 - \cos^2\beta_2}\ . \quad (2)$$

For the central pixel of the hologram with coordinates $(0, 0)$ and the color λ_0 based on the formulas in (2), we obtain the following parameters of the diffraction grating: $(d, \varphi) = (d_0, 0) = (\frac{\lambda_0}{\sin\theta}, 0)$, where $d_0 = \frac{\lambda_0}{\sin\theta}$.

Usually, in practical cases $\theta = 30^0 - 45^0$, for example, if $\theta = 30^0$, the desired interval of spatial frequencies of diffraction gratings for all colors in spectral range $\lambda_0 = 440 - 650\,nm$ will be $f = d_0^{-1} = 1135 - 650\,mm^{-1}$. At the next step, we can define the parameters (d, φ) of a pixel with the coordinates (x, y) having the same visual characteristics (color, brightness) for the observer as in the case of the central pixel.

This requires solving a system of equations for the variables d and φ:

$$\cos\alpha_2 = -\frac{\lambda_0 \sin\varphi}{d};\ \cos\beta_2 = -\sin\theta + \frac{\lambda_0\cos\varphi}{d};\ \cos\alpha_2 = -\frac{x}{L};\ \cos\beta_2 = -\frac{y}{L}\ . \quad (3)$$

From the equations in (3) we can find the formulas for calculating the parameters of diffraction gratings of the pixel:

$$tg\,\varphi = -\frac{\cos\alpha_2}{\cos\beta_2 + \sin\theta} \quad \Rightarrow \quad \varphi(x,y) = arctg\left\{\frac{x}{L\sin\theta - y}\right\} \quad (4)$$

$$d = -\frac{\lambda_0 \sin\varphi}{\cos\alpha_2} \quad \Rightarrow \quad d(x,y) = \frac{d_0\, L\sin\theta}{\sqrt{(L\sin\theta - y)^2 + x^2}} \quad (5)$$

The size of security holograms is usually not bigger than 3x3 cm and corresponds to the conditions $z >> x$ and $z >> y$; in this case, the following simplified formulas can be used for calculations:

$$d(x,y) \approx \frac{d_0}{1-\frac{y}{z\sin\theta}}, \text{ or the equivalent } f(x,y) = \frac{1}{d(x,y)} \approx f_0\left(1-\frac{y}{z\sin\theta}\right), \text{ where } f_0 = d_0^{-1} \quad (6)$$

and

$$\varphi(x,y) \approx \frac{x}{z\sin\theta - y}, \quad (7)$$

with the distance from hologram to observer, as mentioned above, $z \approx 30\,cm$.
In the extreme case, when $z \to \infty$ (or $x^2 + y^2 \to 0$) equations (6 and 7) become quite simple:

$$d(x,y) \approx d_0 \text{ and } \varphi(x,y) \approx 0 \quad (8)$$

Equations (8) can be used for holograms of up to 1.5x1.5 cm in size, with holograms of larger sizes demonstrating a noticeable color distortion and irregularity of the brightness of pixels in the hologram area.
In the photos presented in Fig.24, one can see two holograms of the same size recorded on the basis of the same original image, a uniform background of a certain color. In case of Fig.24a, calculation was made according to the formulas in (8), and in case of Fig.24b, taking into account the formula in (7). It is clearly seen that in the first case, the brightness of pixels in the direction of observation strongly depends on the position of pixels in the hologram.

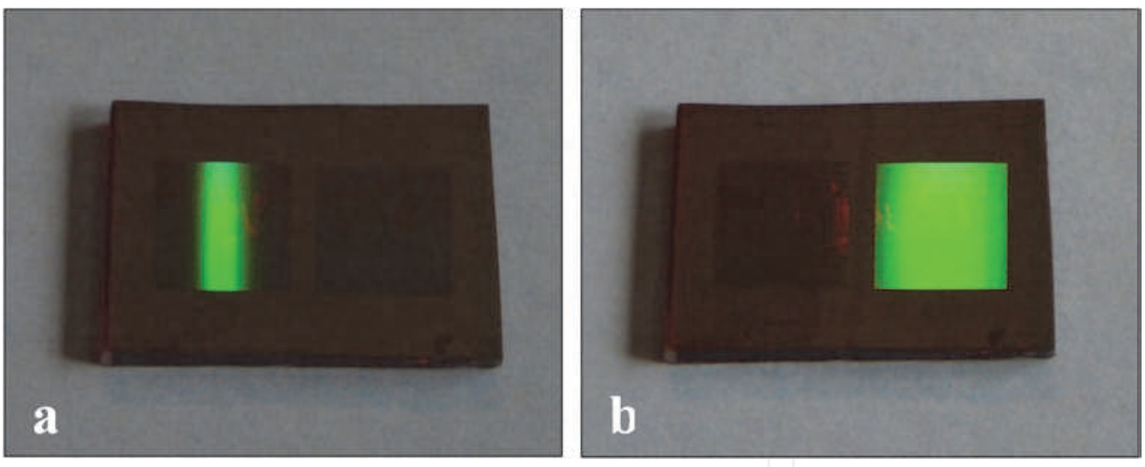

Fig. 24. Photos of a recovered image from a dot-matrix hologram recorded on $As_{40}S_{20}Se_{40}$ photoresist. a) Orientation angle of diffraction grating of all pixels $\varphi = 0$
b) Orientation angle of diffraction grating depending on the position of pixels $\varphi = K\,x$

Calculation of pixel parameters for stereograms or kinematic effects is similar to the considered case. It is only necessary to take into account a new position of observation of the hologram that can be achieved by replacing the old variables (x,y) in formulas (4)-(7) by the new ones $(x-\Delta x, y-\Delta y)$, where $(\Delta x, \Delta y)$ indicate displacement of the observer in the observation plane.

7. Conclusion

The developed and assembled optical devices for dot-matrix holographic and image-matrix recording have been successfully used for scientific purposes as well as for producing holograms for the protection and identification of industrial products and documents. Its compact dimensions, reliability and low cost price may be interesting for the needs of small and medium size business enterprises.

The possibilities of hologram recording on As-S-Se chalcogenide films have been studied. The obtained results show that the above mentioned chalcogenides may be successfully used in applied dot-matrix and image-matrix holography as an excellent alternative to organic photoresists for producing high-quality security holograms with high diffraction efficiency up to 65%. The increase in film sensitivity with increase of the exposure power density has been discovered. It makes the application of pulse recording attractive.

8. Acknowledgments

This research was partly supported by the ESF project "Starpdisciplinārās zinātniskās grupas izveidošana jaunu fluorescentu materiālu un metožu izstrādei un ieviešanai" Nr. 2009/0205/1DP/1.1.1.2.0/09/APIA/VIAA/152

9. References

Pizzanelly D. (2004). The development of direct-write digital holography. Technical review, Holographer.org.

Teteris J. (2002). Holographic recording in amorphous chalcogenide semiconductor thin films, JOAM Vol.4, No. 3, 687.

Teteris J. (2003). Holographic recording in amorphous chalcogenide thin films. Current Opinion in Solid State and Materials Science 7, 127.

Chih-Kung L., Wen-Jong W., Sheng-Lie Y., (2000) Optical configuration and color representation range of a variable-pitch dot matrix holographic printer. Applied Optics Vol.39, No.1, 40.

Yaotang.L, Tianji W., Shining Y., Shining Y., Shichao Z. (1998). Theoretical and experimental study of dot matrix hologram, Proc. SPIE Vol. 3569, 121.

Frumar M., Cernosek Z., Jedelsky J., Frumarova B., Wagner T. (2001). Photoinduced changes of structure and properties of amorphous binary and ternary chalcogenides, JOAM Vol.3, No. 2, 177.

Ozols A.,Reinfelde M., Nordman O. (2001). Photoinduced Anisotrophy and holographic recording in amorphous chalcogenides, Proc. of SPIE Vol.4415

Reinfelde M., Teteris J., Kuzmina I. (2003). Amorphous As-S-Se films for holographic recording. Proc. of SPIE Vol.5123, 128.

Kostyukevych S. Moskalenko N. (2001). Using non-organic resist based on As-S-Se chalcogenide glasses for combined optical/digital security devices, Semiconductor Physics, Quantum Electronics & Optoelectronics, Vol.4, N 1, 70.

Kohler C., Schwab X., (2006). Optimally tured sptial light modulators for digital holography, Applied Optics, Vol.45, No.5, p. 960-967

Gerbreders V., Teteris J., Sledevskis E. (2007). Photoinduced changes of optical reflectivity in As_2S_3-Al system, JOAM, Vol.9, No.10, 3153.

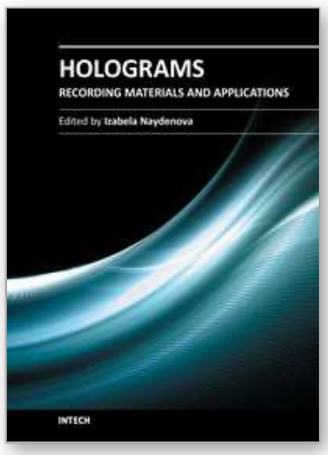

Holograms - Recording Materials and Applications

Edited by Dr Izabela Naydenova

ISBN 978-953-307-981-3
Hard cover, 382 pages
Publisher InTech
Published online 09, November, 2011
Published in print edition November, 2011

Holograms - Recording Materials and Applications covers recent advances in the development of a broad range of holographic recording materials including ionic liquids in photopolymerisable materials, azo-dye containing materials, porous glass and polymer composites, amorphous chalcogenide films, Norland optical adhesive as holographic recording material and organic photochromic materials. In depth analysis of collinear holographic data storage and polychromatic reconstruction for volume holographic memory are included. Novel holographic devices, as well as application of holograms in security and signal processing are covered. Each chapter provides a comprehensive introduction to a specific topic, with a survey of developments to date.

InTech Europe
University Campus STeP Ri
Slavka Krautzeka 83/A
51000 Rijeka, Croatia
Phone: +385 (51) 770 447
Fax: +385 (51) 686 166
www.intechopen.com

InTech China
Unit 405, Office Block, Hotel Equatorial Shanghai
No.65, Yan An Road (West), Shanghai, 200040, China
中国上海市延安西路65号上海国际贵都大饭店办公楼405单元
Phone: +86-21-62489820
Fax: +86-21-62489821

IntechOpen